NASA TECHNICAL NOTE

NASA TN D-3820

C. 1

NASA TN D-3820

STRESS INTENSITY FACTORS FOR CRACKLINE-LOADED EDGE-CRACK SPECIMENS

by John E. Srawley and Bernard Gross

Lewis Research Center
Cleveland, Ohio

NATIONAL AERONAUTICS AND SPACE ADMINISTRATION • WASHINGTON, D. C. • FEBRUARY 1967

NASA TN D-3820

STRESS INTENSITY FACTORS FOR CRACKLINE-LOADED EDGE-CRACK SPECIMENS

By John E. Srawley and Bernard Gross

Lewis Research Center
Cleveland, Ohio

NATIONAL AERONAUTICS AND SPACE ADMINISTRATION

For sale by the Clearinghouse for Federal Scientific and Technical Information
Springfield, Virginia 22151 – Price $1.00

STRESS INTENSITY FACTORS FOR CRACKLINE-LOADED EDGE-CRACK SPECIMENS

by John E. Srawley and Bernard Gross

Lewis Research Center

SUMMARY

Crackline-loaded edge-crack specimens are flat plate specimens which have a single crack notch extending normally from one edge and which are loaded in tension at positions close to the intersection of the crack with that edge. These specimens are of interest in fracture-mechanics testing because they require comparatively little material and because there are some varieties for which the stress intensity factor K is almost independent of crack length over a considerable range.

Stress intensity factors were determined for a variety of these specimens, all with straight boundaries, by boundary collocation of the Williams form of stress function. The boundary conditions were determined with the aid of another stress function due to Filon. The results presented are considered to be comprehensive enough for a wide variety of applications of these specimens.

Two complementary types of semifinite crackline-loaded specimen are treated in detail. The results for these specimens can be used graphically to obtain a useful preliminary estimate of the results for any finite specimen with straight boundaries. Boundary collocation analysis need then be conducted only on those cases which appear to be of most practical interest.

The boundary collocation results were used to calculate values of the stress intensity coefficient $KBW^{1/2}/P$ for a crackline-loaded specimen of nonlinear contour. These values are in excellent agreement with the published experimental compliance data for this specimen configuration.

INTRODUCTION

The expression "crackline-loaded edge-crack specimens" refers to members of that class of flat plate specimens which have a single crack notch extending normally

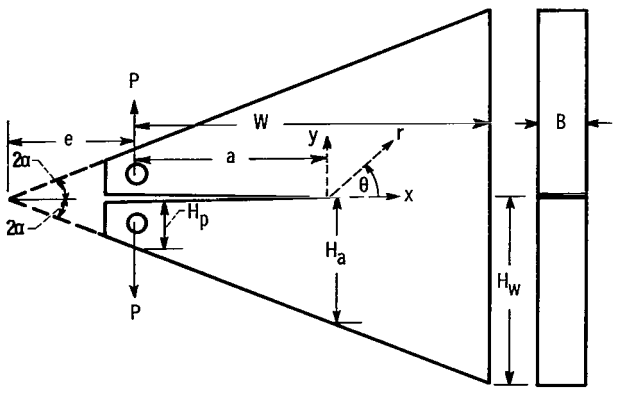

Figure 1. - Crackline-loaded edge-cracked specimen.

from one edge and which are loaded by opposed forces acting parallel to that edge, applied at positions close to the edge and also close to the crackline. The specimens discussed in this report have straight boundaries with slopes H_p/e (= tan 2α), figure 1, varying from 0 to 0.6. It should be noted that the convention used herein is that the dimensions a, e, and W, which are in the direction of the crackline, are measured from the line of action of the load P, not from the actual edge of the specimen. In a previous report (ref. 1) we presented stress intensity factors obtained by boundary collocation for one subclass of these specimens, namely, semifinite specimens (extending indefinitely beyond the crack tip) of zero slope. Detailed information concerning the use of crack-notch specimens for fracture-mechanics tests of materials is contained in references 2 to 7.

There are two aspects of crackline-loaded edge-crack specimens that are of particular interest in connection with fracture-mechanics tests of materials and which led us to conduct a more comprehensive investigation of the relation between stress intensity factors and crack length for such specimens. First, when used for plane strain crack toughness K_{Ic} tests, specimens of this type can be designed so that they require less material per test than any type of remotely loaded specimen (ref. 2). In tests of tough materials of moderate yield strength, the required dimensions of specimens are a major limitation in determination of K_{Ic}. The first such compact crackline-loaded specimen appears to have been that designed by M. J. Manjoine (ref. 3), which has since been extensively used and studied (refs. 4 to 6). The current modifications of Manjoine's design are commonly called WOL (wedge-opening-loaded) specimens.

The second attractive feature of crackline-loaded edge-crack specimens is that they can be shaped in such a way that the stress intensity per unit load is practically independent of crack length over a substantial range. This feature can be a valuable asset, for instance, in fatigue crack-propagation experiments or environmentally influenced crack-propagation experiments because the stress intensity can be controlled simply by controlling the load without regard to the crack length. The advantage of shaping specimens in this way was first brought to our attention by E. J. Ripling in 1964, and the results of his experimental studies with such specimens have since been reported (ref. 7).

Although stress intensity calibrations of good accuracy have been published for a few special cases of crackline-loaded specimens (refs. 1, 4, and 7), we nevertheless considered that a broad parametric study of the general specimen type would be valuable as a basis for judicious selection of specimen dimensions for specific purposes. The results

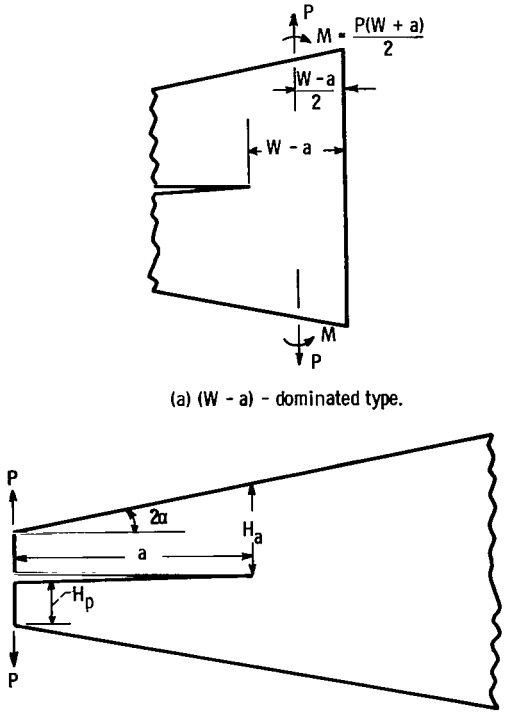

(a) (W - a) - dominated type.

(b) (W - a) - indifferent type.

Figure 2. - Complementary types of semifinite specimen.

reported herein were obtained by the boundary collocation procedure that we have applied previously to other specimen configurations (refs. 1, 8, 9, and 10). This procedure is used to determine the coefficient of the first term of a Williams form of stress function (refs. 11 and 12), which is proportional to the stress intensity factor K. The necessary boundary conditions for the tapered specimens were determined by another stress function from Filon and Coker (ref. 13).

It is possible to get a good general impression of the dependence of the stress intensity factor on the crack length for different values of the specimen shape parameters (H_p, e, and W, or an equivalent set) by considering the two complementary types of semifinite specimen shown in figure 2. In one type, the distance W - a from the crack tip to the normal boundary is small compared with the crack length and with the distance to a transverse or oblique boundary. The crack-tip stress field is then dominated by the proximity of the normal boundary. It is convenient to refer to this case as the (W - a)-dominated type of semifinite specimen. There is an expression for a semifinite crack approaching the free edge of a half-plane given in the compilation by Paris and Sih (ref. 14, eq. (181)) which can be adapted to this case. The complementary type of semifinite specimen is that in which the normal boundary is far enough from the crack tip that its position has negligible effect on the crack-tip stress field. This type is referred to as the (W - a)-indifferent type of semifinite specimen. This case was treated in reference 1 for specimens with zero taper (H constant), and it was shown that the dependence of $KBH^{1/2}/P$ on a/H is linear. The present boundary collocation results show that the dependence of $KBH_a^{1/2}/P$ on a/H_a, where H_a is the vertical height of the specimen arm at the crack tip, is also linear when the taper is not zero. Approximate treatment of these specimens as double cantilevers (refs. 7, 15, and 16) was not sufficiently accurate for our purpose, for reasons discussed in the appendix.

Our purpose in considering the two types of semifinite specimens was to reduce to a minimum the number of boundary value computations that it was necessary to carry out. In conjunction with a moderate number of boundary collocation results to establish the necessary numerical coefficients, the semifinite relations can be used to sketch out the multidimensional field of the values of the stress intensity coefficient $KBW^{1/2}/P$ with useful accuracy. Further computational effort could then be concentrated on those spec-

imen shapes which are of most practical interest, as indicated by the preliminary results.

SYMBOLS

Units may be in any consistent system, since only dimensionless combinations are used in this report.

a	effective crack length
B	specimen thickness
d_{2n}, d_{2n-1}	coefficients of Williams stress function
e	distance from wedge tip to line of load application
H	uniform depth of nontapered split arm
H_a	depth of tapered split arm at crack tip a
H_p	depth of tapered split arm at load line
H_w	depth of tapered split arm at end boundary location
H_δ	depth of tapered split arm at location δ
K_I	stress intensity factor of elastic stress field in the vicinity of the crack tip
K_{Ic}	critical value of K at point of instability of crack extension in first or opening mode, a measure of plane strain crack toughness of material
M	bending moment
m	number of selected boundary stations for collocation solution
P	load applied to both arms of specimen
r	polar coordinates referred to crack tip
W	specimen width
x, y	cartesian coordinate system referred to crack tip
α	half-angle of taper, 1/2 arctan (H_p/e)
δ	distance measured from load line to new end boundary location
ζ	normal direction to all boundaries
η, ξ	cartesian coordinate system referred to wedge tip
θ	polar coordinate referred to crack tip
ρ	polar coordinate referred to wedge tip
ρ_C	distance from wedge apex to location C

σ_x	stress component in x-direction
σ_y	stress component in y-direction
τ_{xy}	shearing stress component
φ	polar coordinate referred to the wedge tip
χ	Airy stress function

BOUNDARY COLLOCATION PROCEDURE

The method of analysis consists in finding a stress function that satisfies the biharmonic equation $\nabla^4\chi = 0$ and also the boundary conditions at a finite number of stations along the boundary of a specimen, such as that shown in figure 1. The biharmonic equation and the boundary conditions along the crack are satisfied by the Williams stress function (refs. 11 and 12). Because of symmetry (fig. 1) the coefficients of the sine terms in the general stress function must be zero; hence,

$$\chi(r,\theta) = \sum_{n=1,2\ldots} \left\{ (-1)^{n-1} d_{2n-1} r^{n+(1/2)} \left[-\cos\left(n - \frac{3}{2}\right)\theta + \frac{2n-3}{2n+1} \cos\left(n + \frac{1}{2}\right)\theta \right] \right.$$

$$\left. + (-1)^n d_{2n} r^{n+1} \left[-\cos(n-1)\theta + \cos(n+1)\theta \right] \right\} \qquad (1)$$

The stresses in terms of χ obtained by partial differentiation are as follows:

$$\left.\begin{aligned}
\sigma_y &= \frac{\partial^2\chi}{\partial x^2} = \frac{\partial^2\chi}{\partial r^2}\cos^2\theta - 2\frac{\partial^2\chi}{\partial\theta\,\partial r}\frac{\sin\theta\cos\theta}{r} + \frac{\partial\chi}{\partial r}\frac{\sin^2\theta}{r} + 2\frac{\partial\chi}{\partial\theta}\frac{\sin\theta\cos\theta}{r^2} + \frac{\partial^2\chi}{\partial\theta^2}\frac{\sin^2\theta}{r^2} \\
\sigma_x &= \frac{\partial^2\chi}{\partial y^2} = \frac{\partial^2\chi}{\partial r^2}\sin^2\theta + 2\frac{\partial^2\chi}{\partial\theta\,\partial r}\frac{\sin\theta\cos\theta}{r} + \frac{\partial\chi}{\partial r}\frac{\cos^2\theta}{r} - 2\frac{\partial\chi}{\partial\theta}\frac{\sin\theta\cos\theta}{r^2} + \frac{\partial^2\chi}{\partial\theta^2}\frac{\cos^2\theta}{r^2} \\
-\tau_{xy} &= \frac{\partial^2\chi}{\partial x\,\partial y} = \sin\theta\cos\theta\frac{\partial^2\chi}{\partial r^2} + \frac{\cos 2\theta}{r}\frac{\partial^2\chi}{\partial r\,\partial\theta} - \frac{\sin\theta\cos\theta}{r^2}\frac{\partial^2\chi}{\partial\theta^2} - \frac{\sin\theta\cos\theta}{r}\frac{\partial\chi}{\partial r} \\
&\qquad - \frac{\cos 2\theta}{r^2}\frac{\partial\chi}{\partial\theta}
\end{aligned}\right\} \qquad (2)$$

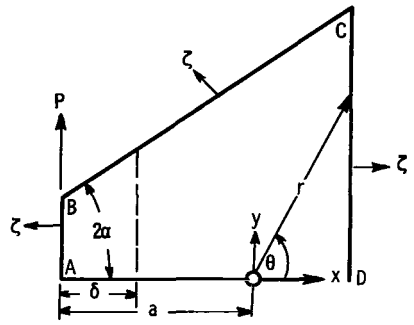

(a) Tapered-beam specimen boundary.

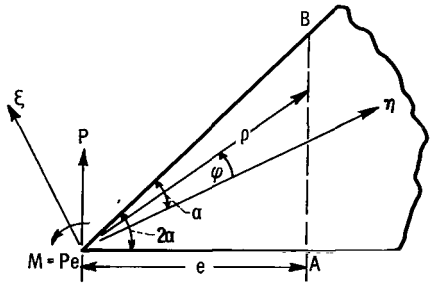

(b) Force diagram about tapered-beam specimen, cantilever tip.

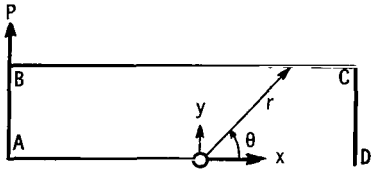

(c) Rectangular-beam specimen boundary.

Figure 3. - Geometric relations used in developing equations (3) and (4).

The boundary collocation procedure consists in solving 2m simultaneous algebraic equations corresponding to the known values of χ and $\partial\chi/\partial\zeta$, where ζ is the variable taken in the direction normal to the boundary (fig. 3(a)) at m selected stations along the boundary ABCD. Values for the first 2m coefficients of the Williams stress function are thus obtained when the remaining terms are neglected. Only the value of the first coefficient d_1 is used for the present purpose since the stress intensity factor K_I is equal to $-\sqrt{2\pi}\, d_1$ as shown in reference 8.

For nonzero values of the angle 2α, the required values of χ and its first derivative at the m selected boundary stations were obtained from the known solution to the wedge problem with loads at the wedge tip (fig. 3(b)) as given in reference 13. The stress function along boundary AB is formulated in the η, ξ plane and is given in terms of the polar coordinates ρ and φ. This stress function may be transformed to rectangular coordinates x, y with origin at the crack tip by the following transformation (fig. 3(c)):

$$x = \rho \cos(\alpha + \varphi) - (e + a) = r \cos\theta$$

$$y = \rho \sin(\alpha + \varphi) = r \sin\theta$$

where r and θ are polar coordinates in the x, y plane. The equations for obtaining the boundary values are as follows:

Along AB,

$$\frac{1}{\rho}\frac{\chi}{P} = \varphi\left(\frac{-\sin\alpha\sin\varphi}{2\alpha + \sin 2\alpha} + \frac{\cos\alpha\cos\varphi}{2\alpha - \sin 2\alpha}\right) + \frac{e}{2\rho}\left(\frac{\sin 2\varphi - 2\varphi\cos 2\alpha}{2\alpha\cos\alpha - \sin 2\alpha} - 1\right)$$

$$+ \cos\varphi\left(\frac{-\sin^3\alpha}{2\alpha + \sin 2\alpha} + \frac{\alpha\cos\alpha - \sin\alpha\cos^2\alpha}{2\alpha - \sin 2\alpha}\right)$$

$$- \sin\varphi\left(\frac{\alpha\sin\alpha + \cos\alpha\sin^2\alpha}{2\alpha + \sin 2\alpha} + \frac{\cos^3\alpha}{2\alpha - \sin 2\alpha}\right)$$

$$-\frac{\partial(\chi/P)}{\partial\zeta} = \frac{\partial(\chi/P)}{\partial x} = \frac{\partial(\chi/P)}{\partial\rho}\cos(\varphi + \alpha) - \frac{1}{\rho}\frac{\partial(\chi/P)}{\partial\varphi}\sin(\varphi + \alpha)$$

Along BC,

$$\frac{1}{\rho}\left(\frac{\chi}{P}\right) = (1 - 2\sin^2\alpha) - \frac{e}{\rho}$$

$$\frac{\partial(\chi/P)}{\partial\zeta} = -\sin 2\alpha$$

Along CD,

$$\frac{1}{\rho_C}\left(\frac{\chi}{P}\right) = (1 - 2\sin^2\alpha) - \frac{e}{\rho_C}$$

$$\frac{\partial(\chi/P)}{\partial\zeta} = \frac{\partial(\chi/P)}{\partial x} = \frac{\partial(\chi/P)}{\partial\rho}\cos 2\alpha - \frac{1}{\rho}\frac{\partial(\chi/P)}{\partial\varphi}\sin 2\alpha = 1$$

(3)

where ρ_C is the distance from wedge apex to location C.

The distance from the collocation boundary AB to the crack tip (the distance $a - \delta$ in fig. 3(a)) was varied for computational convenience. For δ equal to zero, the resultant bending moment at boundary AB is zero, and the resulting shear force is equal to the applied load P. It is obvious that the boundary AB should not be taken too close to the crack tip on the basis of the St. Venant principle.

A typical plot of the shear stress τ_{xy} and normal stress σ_x distributions along boundary AB ($\delta = 0$) resulting from the stress function solution to the wedge problem is

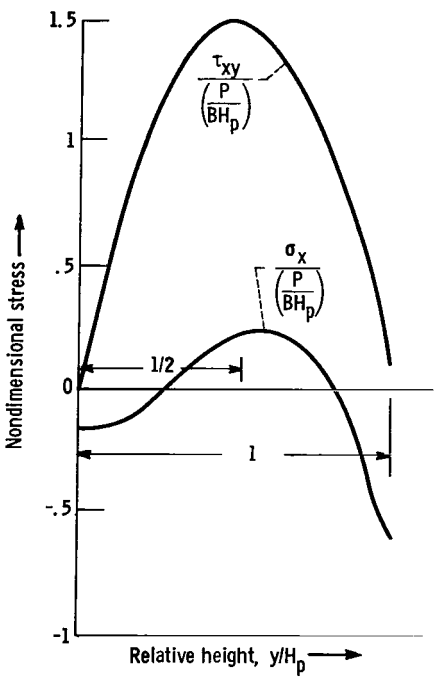

Figure 4. - Distribution of stresses σ_x and τ_{xy} at x = -a (fig. 3) based on stress function solution to wedge problem where P = 1, δ/e = 0, e = 1.5, B = 1, a = 4, W = 6, and H_p/e = 0.20.

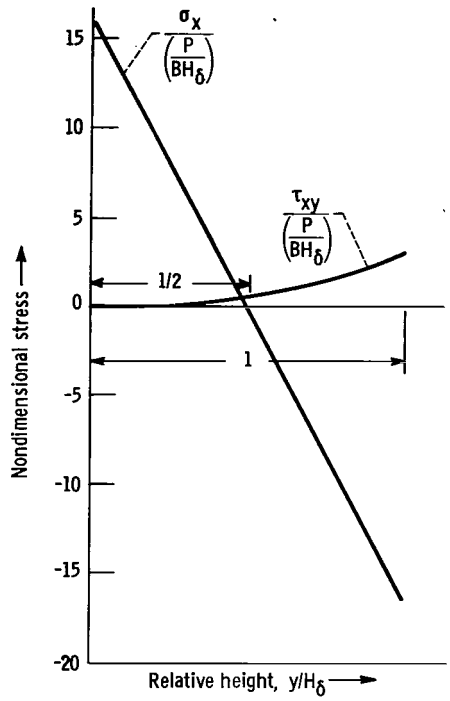

Figure 5. - Distribution of stress σ_x and τ_{xy} at x = δ - a (fig. 3) based on stress function solution to wedge problem where P = 1, δ/e = 1.07, e = 1.5, B = 1, a = 4, W = 6, and H_p/e = 0.20.

shown in figure 4. At this location, the resultant bending moment is equal to zero, and the shear load is equal to P. While the shear distribution τ_{xy} at location AB is similar to that resulting from simple beam theory, a small residual normal stress distribution σ_x occurs in the stress function solution.

A typical plot of stress distribution when δ in not equal to zero is shown in figure 5. The normal stress distribution σ_x is very nearly the same as that obtained using simple beam theory, but the shear stress distribution is quite different.

The stress intensity values obtained when δ was taken to be different from zero were identical with those obtained for δ equal to zero.

For the special case of the rectangular specimen (H_p finite and 2α equal to zero) as shown in figure 3(c), the equations for obtaining the boundary values are as follows:

Along AB,

$$\frac{\chi}{P} = \frac{-6(a + x)}{BH_p^3}\left(\frac{y^3}{3} - \frac{H_p y^2}{2}\right)$$

$$-B\frac{\partial(\chi/P)}{\partial\zeta} = B\frac{\partial(\chi/P)}{\partial x} = \frac{-6}{BH_p^3}\left(\frac{y^3}{3} - \frac{H_p y^2}{2}\right)$$

Along BC,

$$\frac{\chi}{P} = \frac{x + a}{P}$$

$$B\frac{\partial(\chi/P)}{\partial\zeta} = B\frac{\partial(\chi/P)}{\partial y} = 0$$

Along CD,

$$\frac{\chi}{P} = \frac{W}{B}$$

$$B\frac{\partial(\chi/P)}{\partial\zeta} = B\frac{\partial(\chi/P)}{\partial x} = 1$$

(4)

The boundary stations were equally allocated among the three boundaries; the spacing was uniform along each boundary. The collocation computations were carried out for each set of selected values of the primary variable a/H_p and the parameters 2α and W/H_p. In general, the number of boundary stations m varied from 18 to 45.

RESULTS AND DISCUSSION

Preliminary Results for Semifinite Specimens

As mentioned in the INTRODUCTION, the complete field of values of the stress intensity factor K can be derived with fair accuracy from a knowledge of the characteristics of the two semifinite specimens shown in figure 2. Equation (181) of reference 14 can be

adapted to the (W - a)-dominated type of semifinite specimen by reformulating the relation in terms of a crack length a and a specimen width W. The result can then be expressed conveniently in terms of the dimensionless stress intensity coefficient $KBW^{1/2}/P$:

$$\frac{KBW^{1/2}}{P} = \frac{0.537 + 2.17(1 + a/W)/(1 - a/W)}{(1 - a/W)^{1/2}} \tag{5}$$

There are several other forms of dimensionless stress intensity coefficient (for instance, $KBH_P^{1/2}/P$), but the selected form has the advantage that it is a single valued function of a/W for all values of the parameters H_p/e and W/e. Furthermore, it is appropriate for practical use since the measurement of W is more direct than the measurement of H_p or H_a and has to be made in any case.

To obtain quantitative expressions for the (W - a)-indifferent semifinite specimens of various slopes H_p/e, it was first necessary to obtain some appropriate boundary collocation results. The method proposed in references 7, 15, and 16 for deriving such expressions by treating the specimen as a pair of cantilevers was not satisfactory (see appendi). When the necessary boundary collocation results are expressed in terms of $KBH_a^{1/2}/P$ and a/H_a as in figure 6, it is seen that they are a very good fit to a family of straight lines with slopes Λ that depend upon H_p/e. These lines appear to have a common origin at $a/H_a \simeq -0.7$. We can offer no simple explanation of this apparently simple finding; indeed, we suspect that the linear relations would not apply to actual specimens with sufficiently small a/H_a. It must be remembered that the assumption of the St. Venant principle is implicit in the application of the boundary collocation method, and this principle is violated for small a/H_a. Satisfactory results could not be obtained by the boundary collocation procedure for (W - a)-indifferent semifinite specimens with H_p/e greater then 0.4, presumably because of the limitations of the computer program. It seemed reasonable, however, to obtain approximate values of the coefficient Λ for H_p/e up to 0.6 by extrapolation of the values that were obtained.

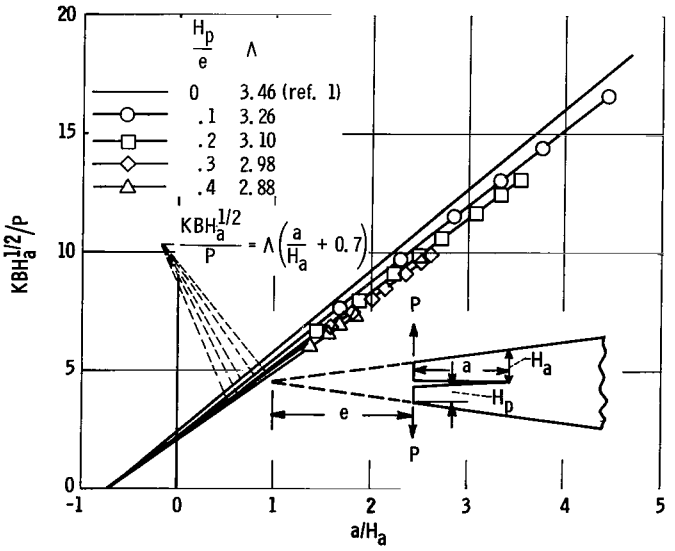

Figure 6. - Boundary collocation results for (W - a) - indifferent semifinite specimens. Coefficients Λ of linear fitting expressions are also shown.

To show the relations for the two semifinite specimen types on a common

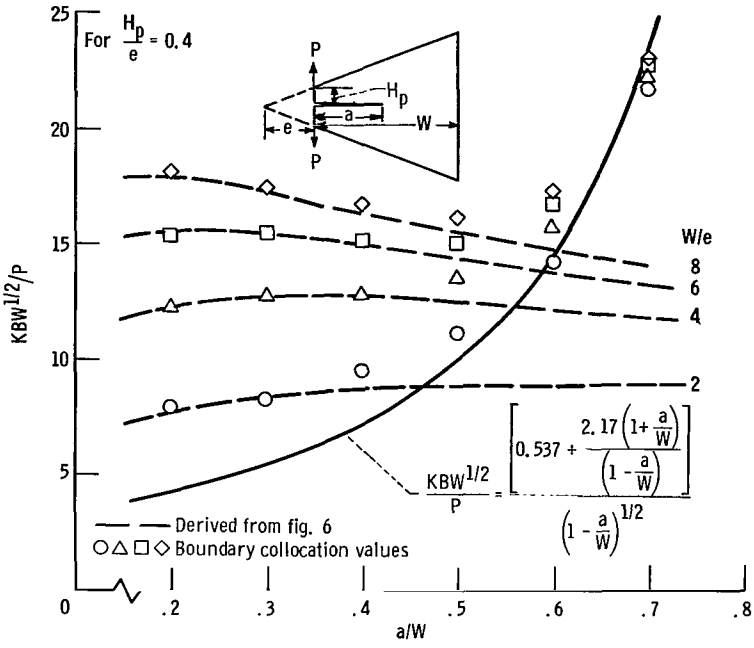

Figure 7. - Example of combined plot for two types of semifinite specimen.

plot, the linear relations between $KBH_a^{1/2}/P$ and a/H_a for the (W - a)-indifferent specimens are readily converted to relations between $KBW^{1/2}/P$ and a/W with parameters H_p/e and either W/e or W/H_p. These latter relations are not linear except when $H_p/e = 0$. An example of a combined plot for the two types of semifinite specimen is shown in figure 7 ($H_p/e = 0.4$). Individual boundary collocation results are also plotted on this figure to show how well they fit the curves. The agreement with the (W - a)-indifferent curves is good in the lower range of a/W, and there is fair agreement with the (W - a)-dominated curve when a/W = 0.7. In the intermediate transition regions the boundary collocation results fall above both applicable curves. It is possible to construct a simple combination function which fits all the results fairly well, but there is little real point to doing so.

By considering superimposed curves such as are shown in figure 7, we were able to select certain combinations of values of H_p/e and W/e which seemed to be of most potential interest. For each combination, we conducted boundary collocation analyses for values of a/W from 0.2 to 0.7 at intervals of 0.1. The results in terms of $KBW^{1/2}/P$ are given in table I.

Comparison With Experimental Results of Mostovoy et al.

Experimental compliance measurement results are given in reference 7 for a speci-

TABLE I. - RESULTS OF BOUNDARY

COLLOCATION COMPUTATIONS

H_p/e	W/e	W/H_p	For a/W values of -					
			0.2	0.3	0.4	0.5	0.6	0.7
			$KBW^{1/2}/P$					
0	0	1.25	-----	5.31	6.86	9.29	13.44	21.52
		1.5	-----	5.59	7.10	9.45	13.52	21.54
		2	5.32	6.49	8.01	10.20	13.92	21.68
		3	7.65	9.35	11.34	13.53	16.64	23.16
		4	10.20	13.00	15.76	18.57	22.35	26.81
		5	12.90	16.85	20.72	24.49	28.61	33.42
		>5	(a)	(a)	(a)	(a)	(a)	(a)
0.1	3	30	63.4	70.5	74.0	75.5	76.1	75.5
	4	40	79.0	85.2	88.0	87.5	86.5	84.5
	5	50	92.5	98	99	97	95	92
0.2	2	10	17.65	20.0	21.3	22.2	23.3	27.0
	3	15	24.5	26.7	27.9	28.1	28.3	30.5
	3.2	16	27.0	28.3	29.0	29.0	29.1	31.0
	4	20	30.3	32.1	32.8	32.2	31.8	33.0
	5	25	35.2	36.2	36.0	35.3	34.5	35.0
0.3	3	10	14.7	15.7	16.1	16.4	18.0	23.5
	3.6	12	16.8	17.5	17.7	17.8	19.0	24.0
	4.2	14	18.6	19.1	19.2	18.94	19.77	24.44
	4.8	16	20.1	20.4	20.2	19.85	20.46	24.82
	5.4	18	21.5	21.6	21.1	20.6	21.0	25.14
	6	20	22.9	22.8	21.9	21.4	21.6	25.4
0.4	3	7.5	10.2	11.0	11.5	12.5	15.1	22.0
	4	10	12.4	12.8	12.9	13.6	15.8	22.3
	5	12.5	14.0	14.2	14.2	14.4	16.3	22.6
	6	15	15.4	15.5	15.2	15.1	16.8	22.8
	8	20	18.2	17.5	16.8	16.2	17.4	23.0
0.5	4	8	-----	9.8	10.3	11.4	14.5	21.8
	5	10	-----	11.2	11.0	11.9	14.7	21.9
	6	12	-----	12	11.6	12.5	15.0	22.0
	8	16	-----	14	12.8	13.2	15.5	22.1
0.6	3	5	-----	7	-----	9.8	13.9	21.5
	4	6.67	-----	-----	7.7	10	14.0	21.6
	5	8.333	-----	-----	-----	10.9	14.1	21.6
	6	10	-----	10	-----	11	14.2	21.7

[a]Use equation in fig. 6 or ref. 1.

TABLE II. - CALCULATED VALUES OF $KBW^{1/2}/P$

FOR SPECIMEN OF REFERENCE 7

a/W	a/H_a	H_p/e	Λ	$KBH_a^{1/2}/P$	$KBW^{1/2}/P$	Experimental result from ref. 7
0.2	1.04	0.53	2.78	4.85	11.1	10.9
.3	1.225	.53	2.78	5.35	10.8	10.9
.4	1.36	.45	2.84	5.87	10.8	10.9
.5	1.50	.45	2.84	6.26	10.8	10.9

men which was contoured so that the stress intensity per unit load would be independent of crack length over a substantial range. It is of interest to compare these experimental results with the present results for (W - a)-indifferent specimens. The comparison is most conveniently made in terms of the stress intensity coefficient $KBW^{1/2}/P$. For the specimen of reference 7, the inferred value of $KBW^{1/2}/P$ is 10.9 for all values of a/W between 0.18 and 0.55. The equation shown in figure 6 was used to calculate comparison values by the method of the previous section. To do this it was necessary to interpolate values of the coefficient Λ on the basis of values of H_p/e calculated from the dimensions of the specimen of reference 7. (The exact dimensions are not given in the reference; they were provided to us by the authors.) The results are given in table II and agree very well with the experimental result.

Final Results for Selected Specimens

The precision of each result in table I is indicated in each case by the number of significant figures to which the value of $KBW^{1/2}/P$ is given. The last digit is precise to within three units or less. Precision here refers to the variation of successive boundary collocation results with successive increase in the number of collocation stations beyond some minimum number. Some discretion has been excercised, however, in rejecting seemingly obviously disparate results which occurred occasionally in most runs. The precision is quite variable, and there are some blanks in the table where no useful result could be obtained. The results for $H_p/e = 0.6$ are the least satisfactory, and this slope appears to represent about the limit of capability of our computer program.

For all values of H_p/e except zero, there are certain combinations of ranges of W/e and a/W in which $KBW^{1/2}/P$ passes very gradually through a maximum or an inflexion. As mentioned in the INTRODUCTION, such ranges of almost constant $KBW^{1/2}/P$ are of considerable interest for certain experimental purposes. Several examples, selected from table I, are shown in figure 8. Clearly, there is a number of al-

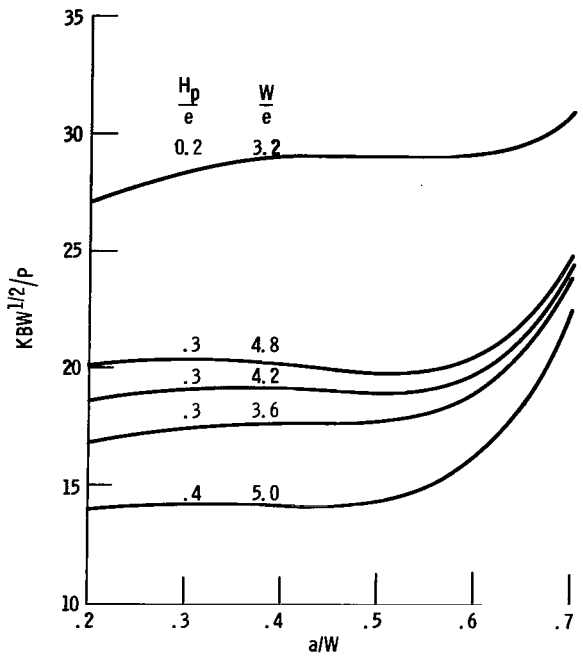

Figure 8. - Selection of curves of $KBW^{1/2}/P$ and a/W for tapered specimens of such proportions that K is almost independent of a over a substantial range.

ternative possibilities, and selection from among these for a particular purpose will depend on other considerations which are outside the scope of this report. One thing that should be realized, however, is that the proportions of all the "constant-$KBW^{1/2}/P$" specimens in table I are such that the forward direction of crack propagation is unstable. Reference 7 should be consulted for further information on this point and for guidance regarding the use of face grooves (or side notches) to circumvent this difficulty.

For rectangular specimens (W/e = 0), $KBW^{1/2}/P$ increases more rapidly with a/W the higher the value of a/W, for all values of W/H_p. Again, practical considerations will determine the choice of proportions of a rectangular specimen for a given purpose. For K_{Ic} tests, there are two factors which strongly favor the choice of a relatively compact specimen (W/H_p about 2). These factors are (a) economical use of material and (b) avoidance of the need for face grooving of the specimen to control the direction of propagation of the crack (ref. 2).

CONCLUSION

The boundary collocation results given in this report for specimens with straight boundaries appear to us to be sufficiently comprehensive for applications which we can forsee. Should more extensive results be needed, it is a simple matter to apply the results for the two types of semifinite specimen to obtain a useful idea of the behavior of the appropriate dimensionless stress intensity coefficient in the region of interest. The boundary collocation method can then be applied to obtain more precise results for specific cases. In this connection, the pattern of the precision of the boundary collocation results given herein provides an indication of where the method is most effective and where it is least effective.

Lewis Research Center,
National Aeronautics and Space Administration,
Cleveland, Ohio, November 8, 1966,
731-21-03-03-YBG0615.

APPENDIX - APPROXIMATE TREATMENT OF CRACKLINE-LOADED EDGE-CRACK SPECIMENS AS PAIRS OF CANTILEVER BEAMS

Several treatments (refs. 7, 15, and 16) have been published in which the relative deflection of the arms of a (W - a)-indifferent type of semifinite specimen is calculated by the methods commonly described in texts on strength of materials. The result is used to determine the energy release rate with crack extension $\mathcal{G}$ from the Irwin-Kies relation (ref. 17):

$$\mathcal{G} = \frac{P^2}{2B^2} \frac{d}{da} (2vB/P) \tag{A1}$$

where $2v$ is the relative displacement of the points of application of the load P. The stress intensity factor is given by

$$K^2 = E\mathcal{G} \tag{A2}$$

(for generalized plane stress, which is appropriate for a planar model).

Since we were not able to obtain sufficiently accurate preliminary results by this method, it is useful to indicate its limitations.

For small deflections, the local curvature of each arm of the rectangular specimen shown in figure 9 is

$$\frac{d^2y}{dx^2} = \frac{P(a - x)}{EI} = \frac{12P(a - x)}{EBH^3} \tag{A3}$$

and the slope at any point is

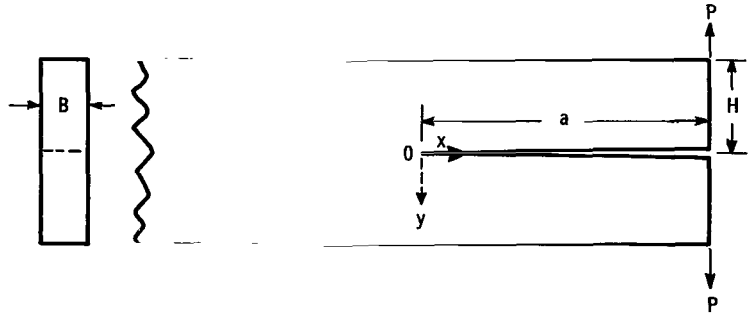

Figure 9. - Rectangular (W - a) - indifferent type of semifinite crackline-loaded edge-crack specimen.

$$\frac{dy}{dx} = \frac{12P}{EBH^3}\left[\int_0^x (a - x)dx + I_o(a, H)\right] = \frac{12P}{EBH^3}\left(ax - \frac{x^2}{2} + I_o\right) \tag{A4}$$

where I_o is the initial slope at 0 and is a function of a and of H, which cannot be determined by elementary methods because of the singular nature of the stress field at the crack tip. The deflection of the point of load application relative to the origin is, therefore,

$$y_{(x=a)} = v = \frac{12P}{EBH^3}\int_0^a \left(ax - \frac{x^2}{2} + I_o\right)dx = \frac{12P}{EBH^3}\left(\frac{a^3}{2} - \frac{a^3}{6} + I_o a\right) \tag{A5}$$

and, hence, the compliance C of the specimen is

$$C = \frac{2v}{P} = \frac{24}{EBH^3}\left(\frac{a^3}{3} + I_o a\right) \tag{A6}$$

and

$$\frac{dC}{da} = \frac{24}{EBH^3}\left[a^2 + \frac{d}{da}(I_o a)\right] \tag{A7}$$

therefore, from equations (A1) and (A2),

$$\frac{K^2B^2}{P^2} = \frac{EB}{2}\frac{dC}{da} = \frac{12}{H^3}\left[a^2 + \frac{d}{da}(I_o a)\right] \tag{A8}$$

Since the term $\frac{d}{da}(I_o a)$ is undetermined, this result is of little value unless a useful approximation can be found for the undetermined term. In this connection, it is useful to compare equation (A8) with the fitting equation to the boundary collocation results for the same type of specimen (ref. 1), as given in figure 6 of this report:

$$\frac{KBH^{1/2}}{P} = 3.46\left(\frac{a}{H} + 0.7\right)$$

or

$$\frac{K^2B^2}{P^2} = \frac{12}{H^3}\left(a^2 + 1.4\ aH + 0.5\ H^2\right) \tag{A9}$$

so that $\frac{d}{da}(I_o a)$ is seen to be approximately equal to $1.4\ aH + 0.5\ H^2$, which is by no means negligible compared with a^2, except when a/H is large. This is not the case for specimens treated herein.

Tapered specimens can be treated similarly by taking the angular bisector as the neutral axis of an arm. The analytical manipulation, however, is somewhat complicated. The outcome, as might be expected, is that the method is increasingly inaccurate with increasing specimen taper.

REFERENCES

1. Gross, Bernard; and Srawley, John E.: Stress-Intensity Factors By Boundary Collocation For Single-Edge-Notch Specimens Subject To Splitting Forces. NASA TN D-3295, 1966.

2. Brown, William F., Jr; and Srawley, John E.: Current Status Of Plane Crack Toughness Testing. ASTM Special Technical Publication No. 410, Jan. 1967.

3. Manjoine, M. J.: Biaxial Brittle Fracture Tests. Paper No. 64-Met-3, ASME, May 1964.

4. Wilson, W. K.: Analytical Determination Of Stress Intensity Factors for the Manjoine Brittle Fracture Test Specimen. Rep. No. WERL-0029-3, Westinghouse Research Laboratories, Aug. 1965.

5. Wilson, W. K.: Optimization of WOL Brittle Fracture Test Specimen. Rep. No. 66-1B4-BTLFR-R1, Westinghouse Research Laboratories, Jan. 1966.

6. Wessel, E. T.; and Pryle, W. H.: Investigation Of The Applicability Of The Biaxial Brittle Fracture Test For Determining Fracture Toughness. Rep. No. WERL-8844-11, Westinghouse Research Lab., Aug. 1965.

7. Mostovoy, S.; Crosley, P. B.; and Ripling, E. J.: Use of Crack Line Loaded Specimens for Measuring Plane Strain Fracture Toughness. Materials Research Laboratory, Inc., June 1966.

8. Gross, Bernard; Srawley, John E.; and Brown, William F., Jr.: Stress-Intensity Factors for a Single-Edge-Notch Tension Specimen by Boundary Collocation of a Stress Function. NASA TN D-2395, 1964.

9. Gross, Bernard; and Srawley, John E.: Stress-Intensity Factors for Single-Edge-Notch Specimens in Bending or Combined Bending and Tension by Boundary Collocation of a Stress Function. NASA TN D-2603, 1965.

10. Gross, Bernard; and Srawley, John E.: Stress-Intensity Factors for Three-Point Bend Specimens by Boundary Collocation. NASA TN D-3092, 1965.

11. Williams, M. L.: On The Stress Distribution at the Base of a Stationary Crack. J. Appl. Mech., vol. 24, no. 1, Mar. 1957, pp. 109-114.

12. Williams, M. L.: The Bending Stress Distribution at the Base of a Stationary Crack. J. Appl. Mech., vol. 28, no. 1, Mar. 1961, pp. 78-82.

13. Coker, E. G.; and Filon, L. N. G.: A Treatise on Photo-Elasticity. 2nd ed., Cambridge University Press, 1957.

14. Paris, Paul C.; and Sih, George C.: Stress Analysis of Cracks. Symposium on Fracture Toughness Testing and Its Applications. ASTM Special Technical Publication No. 381. Am. Soc. Testing Mater., 1965, pp. 30-83.

15. Gilman, John J.: Cleavage, Ductility, and Tenacity in Crystals. Fracture; Proceedings of an International Conference on the Atomic Mechanisms of Fracture. B. L. Averbach, et al., eds., MIT Technology Press, 1959, pp. 193-224.

16. Barenblatt, G. I.: The Mathematical Theory of Equilibrium Cracks in Brittle Fracture. Advances in Applied Mechanics. Vol. 7, H. L. Dryden and Th. von Kármán, eds., Academic Press, 1962, pp. 55-129.

17. Irwin, G. R.; and Kies, J. A.: Critical Energy Rate Analysis of Fracture Strength. Welding J. Res. Suppl., vol. 33, 1954, p. 193s.

"The aeronautical and space activities of the United States shall be conducted so as to contribute . . . to the expansion of human knowledge of phenomena in the atmosphere and space. The Administration shall provide for the widest practicable and appropriate dissemination of information concerning its activities and the results thereof."

—NATIONAL AERONAUTICS AND SPACE ACT OF 1958

NASA SCIENTIFIC AND TECHNICAL PUBLICATIONS

TECHNICAL REPORTS: Scientific and technical information considered important, complete, and a lasting contribution to existing knowledge.

TECHNICAL NOTES: Information less broad in scope but nevertheless of importance as a contribution to existing knowledge.

TECHNICAL MEMORANDUMS: Information receiving limited distribution because of preliminary data, security classification, or other reasons.

CONTRACTOR REPORTS: Technical information generated in connection with a NASA contract or grant and released under NASA auspices.

TECHNICAL TRANSLATIONS: Information published in a foreign language considered to merit NASA distribution in English.

TECHNICAL REPRINTS: Information derived from NASA activities and initially published in the form of journal articles.

SPECIAL PUBLICATIONS: Information derived from or of value to NASA activities but not necessarily reporting the results of individual NASA-programmed scientific efforts. Publications include conference proceedings, monographs, data compilations, handbooks, sourcebooks, and special bibliographies.

Details on the availability of these publications may be obtained from:

SCIENTIFIC AND TECHNICAL INFORMATION DIVISION

NATIONAL AERONAUTICS AND SPACE ADMINISTRATION

Washington, D.C. 20546